Hybrid High-efficiency Synchronous Converter using Si IGBT and SiC MOSFET

Il Yang[1], Woo-Joon Kim[2], Tuan-Vu Le[3],
Seong-Mi Park[4], Sung-Jun Park[5], Ancheng Liu[6*]

⟨Abstract⟩

Currently, with the thriving development in the field of solar energy, the widespread adoption of solar grid-connected power conversion systems is rapidly expanding. As the market continues to grow, the efficiency of solar power conversion systems is steadily increasing, while prices are rapidly decreasing. Photovoltaic panels often produce low output voltages, and Boost converters are commonly employed to elevate and stabilize these voltages. They are also utilized for implementing Maximum Power Point Tracking (MPPT), ensuring the full utilization of solar power generation. Recently, synchronous control techniques have been introduced, using controllable switching devices like Si IGBT or SiC MOSFET to replace the diodes in the original circuits. However, this has raised concerns related to costs. This paper offers a compromise solution, considering both the performance and economic factors of the converter. It proposes a hybrid high-efficiency synchronous converter structure that combines Si IGBT and SiC MOSFET. Additionally, the proposed topology has been practically implemented and tested, with results confirming its feasibility and cost-effectiveness.

Keywords : *Photovoltaic Power Generation, Boost Converter, Synchronous Control, Efficiency*

1　Main Author, Dept. of Electrical Engineering, Chonnam University, Doctor Course
　　E-mail: yyil2002@naver.com
2　Co-author, Dept. of Electrical Engineering, Chonnam University, Doctor Course
　　E-mail: gods2woo@naver.com
3　Co-author, G&EPS, Responsible researcher
　　E-mail: tvle@epskorea.kr
4　Co-author, Dept. of Lift Engineering, Korea Lift College, Associate Professor
　　E-mail: seongmi@klc.ac.kr
5　Co-author, Dept. of Electrical Engineering, Chonnam National University, Professor
　　E-mail: sjpark1@jnu.ac.kr
6*　Corresponding Author, Dept. of Electrical Engineering, Chonnam University, Doctor Course
　　E-mail: 1054924519@qq.com

1. Introduction

The development of the electric power industry, the progress of material science, and the deepening of society's understanding of clean energy make abundant solar energy have good application prospects. Photovoltaic power generation is one of the main forms of solar energy utilization, due to the flexible installation and configuration of photovoltaic equipment, as a supplement to the power supply of the power grid, it occupies an increasingly important position in the energy system. In order to fully utilize photovoltaic power generation and provide stable power to the load, it is necessary to add a level of DC converter circuitry to implement maximum power tracking in the photovoltaic cell (PV) backstage. In a grid-connected PV power generation system, in order to match the connected utility grid voltage, the maximum power tracking of the PV also needs to raise its output voltage to the voltage value required for grid connection, which is generally realized by Boost circuits [1-4].

The inductor current of a Boost circuit has two modes, Continuous Current Mode (CCM) and Discontinuous Current Mode (DCM). In the two different operating modes, the expressions of the relationship between the output voltage and current of the Boost circuit and the input voltage and current are different. When using Boost circuits for MPPT of PV, it is necessary to accurately measure their voltage and current parameters as well

as to rely on algorithmic programs to determine the maximum power point. In order to improve the accuracy of the sensor's measurement of the electrical parameters of the Boost circuit and the flexibility of the algorithmic control, it is necessary to set a certain range of inductance values to maintain the Boost circuit in the CCM mode.

When the PV operates under low light conditions, its output current is very small. When controlling a Boost converter to operate in CCM, there are typically two solutions. The first one is to increase the switching frequency. Higher frequencies require smaller inductance values, resulting in a smaller overall size of the converter. However, higher switching frequencies also lead to increased switching losses. The second solution is to increase the inductance value in the circuit, which, in turn, increases the size and cost of the components. To solve this problem, it is considered to replace the diode of the Boost converter with a controllable switching device so that it can always operate in CCM mode [5-8].

The synchronous Boost converter operates without a distinction between CCM and DCM. Therefore, with the average input current being the same, the inductor value in the circuit can be set to a small value, or the inductor values can be set to be the same. A synchronous Boost converter can provide higher conversion efficiency [9-12]. The choice of controllable switching devices has a significant impact on cost and efficiency.

Therefore, this study conducts an analysis by employing a combination of Si IGBT and SiC MOSFET, making full use of the structural characteristics and the efficiency and cost advantages of both Si IGBT and SiC MOSFET [13-15].

2. Principle Analysis

2.1 Conventional Boost Converter

The structure of a conventional Boost converter is shown in Fig. 1, where the circuit relies on controlling the conduction and turn-off of S to realize the function of raising the DC input voltage V_{in} to V_o.

When switch S is turned on, diode V_D experiences a reverse voltage and turns off. During this time, the input power charges inductor L through the switch S. As the inductor current cannot change abruptly, the current through inductor L linearly increases, and the load is powered by the discharging of the output parallel capacitor C. At the end of the switch S conduction state, the current through inductor L reaches its maximum value. At this point, diode V_D experiences a forward voltage, turning it on, and inductor L discharges through diode V_D, the load, and the power source circuit, causing the current through inductor L to linearly decrease.

Depending on whether the inductor L current has dropped to zero by the time of the next switch S conduction pulse, the operational state of the circuit can be classified into two modes: CCM and DCM. While inductor L discharges, it generates a back electromotive force, and this voltage, when added in the same direction as the input voltage, provides power to the load R at the output and the parallel capacitor C through the power supply circuit.

The voltage gain of the Boost circuit varies with the operating state of the circuit. In the CCM state, the voltage gain G_v can be expressed as

$$G_v = \frac{V_o}{V_{in}} = \frac{1}{1-D} \tag{1}$$

The average value of the output voltage U_o depends on the duty cycle D and the DC input voltage U_{in}, and from the (1), it is clear that the voltage gain G_v should be greater than 1. In the DCM state, the voltage gain G_v is expressed as

Fig. 1 Conventional boost converter

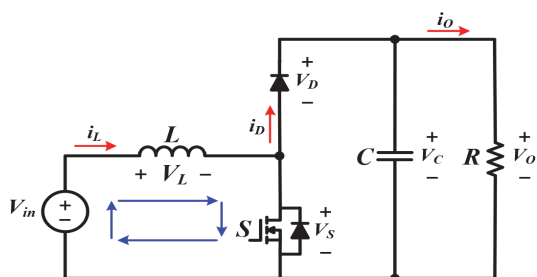$$G_v = \frac{V_o}{V_{in}} = \frac{1}{2}\left(1 + \sqrt{1 + \frac{2D^2 RT_s}{L}}\right) \tag{2}$$

where T_s is the switching period. The average value of its output voltage V_o depends not only on the duty cycle D and DC input voltage V_{in} but also on the output load R, the switching period T_s, and the inductor L.

2.2 Synchronous Boost Converter

The circuit structure of the Boost converter using the synchronous control technique is shown in Fig. 2. As can be seen from the figure, the synchronous Boost circuit consists of two power switching, an input inductor and an output capacitor.

In a synchronous Boost circuit, when both power switches S_1 and S_2 are in the conducting state, the circuit's output parallel capacitor and the load are effectively shorted by S_1 and S_2. Therefore, it is crucial to avoid the simultaneous conduction of S_1 and S_2, which would result in a short circuit. To prevent the concurrent conduction of S_1 and S_2, the synchronous Boost circuit utilizes a complementary drive method with a dead zone. In the complementary drive method, the power switches S_1 and S_2 alternate

between conduction and shutdown.

When S_1 is conducting, and S_2 is off, the input voltage V_{in} passes through S_1, charging inductor L. As the inductor current cannot change abruptly, the current through L linearly increases, and during this time, the load is powered by the discharging of the output parallel capacitor. When S_1 turns off, and S_2 conducts, it operates similarly to a conventional Boost circuit. At the end of the S_1 conduction state, the current through inductor L reaches its maximum value. At this point, the current through L linearly decreases while L discharges, and it generates a back electromotive force. When this voltage is added in the same direction as the input voltage, it provides power to the load at the output and the parallel capacitor through the power supply circuit.

As S_2 conduction state is not affected by changes in the direction of inductor L, the synchronous Boost circuit no longer operates in DCM, and it only functions in CCM. Therefore, the relationship expression for the gain G_v of the synchronous Boost circuit's output voltage concerning the input voltage is:
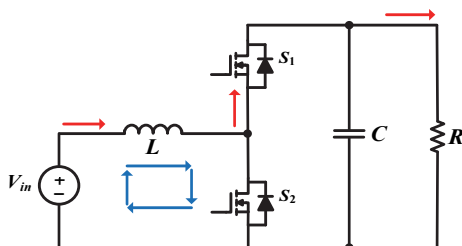
$$G_v = \frac{V_o}{V_{in}} = \frac{1}{1-D} \qquad (3)$$

This article adopts an interleaved delay dead-time control method. precise control of dead time is achieved through the delay mechanisms implemented in the inverter chain of the driving circuit. Regarding the
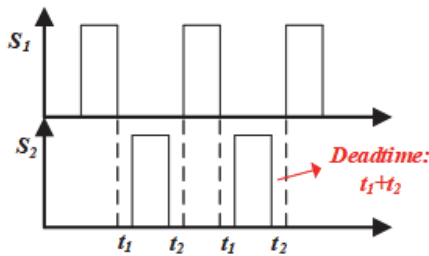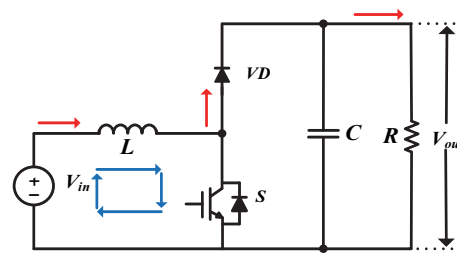

Fig. 2 Synchronous boost converter

Fig. 3 Two switch conduction signal diagram

control of the switching signals, the circuit design allows for turning off siwitch S1, followed by a predetermined delay before turning on switch S2; alternatively, switch S2 can be turned off first, followed by an similar delay before turning on switch S1. The conduction signals of these two switches are depicted in Fig. 3.
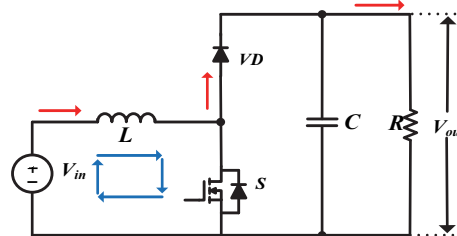
2.3 The Proposed Hybrid High Efficiency Boost Converter

SiC MOSFET offer not only lower conduction losses but also high-speed switching capabilities. SiC MOSFET have a low on-state voltage drop (V_{on}), particularly at low currents. This is attributed to the structural differences between SiC MOSFET and Si IGBT devices. SiC MOSFET as unipolar devices do not have a built-in voltage in the on state, while Si IGBT as bipolar devices do.
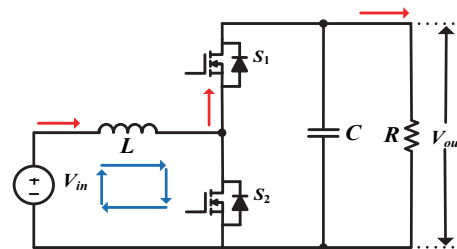
However, SiC MOSFET also encounter some technical challenges, such as misfiring at higher d_v/d_t and d_i/d_t rates, as well as device failures due to surge voltage. Furthermore, under similar product parameters, SiC MOSFET often come at a significantly higher unit cost
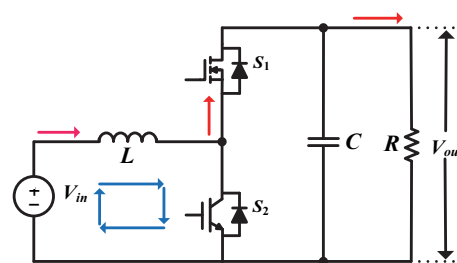

(a) Boost converter based on Si IGBT

(b) Boost converter based on SiC MOSFET

(c) Boost synchronous converter based on SiC MOSFET

(d) Proposed boost synchronous converter

Fig. 4 Types of existing boost converters and the proposed hybrid boost converter

compared to Si IGBT.

Efficiency comparisons and cost analyses were conducted using four different types of Boost converters to validate the proposed

Table 1. Device parameters of MSC015SMA070B, IRGP6690DPbF

	MSC015SMA070B	IRGP6690DPbF
Type	SiC MOSFET	Si IGBT
Manufacturer	Microchip	Infineon
Unite price	41.41$	10.58$
$V_{(BR)DSS}$ (V)	700	600
$I_{D(or\ IC)}$ (A) @TC=25℃	140	140
$R_{DS(ON)}$ (mΩ) @TC=25℃	15	--
$V_{CE(sat)}$ (V) @TJ25℃		1.65

hybrid Boost converter's superior efficiency and lower cost. The Fig. 4. illustrates the structures of the four different Boost converter types.

In a situation where the breakdown voltage and rated current are nearly identical, this paper has chosen Microchip's SiC MOSFET MSC015SMA070B and Infineon's Si IGBT IRGP6690DPbF. Table 1. provides the basic device parameters for both.

Based on Table 1, it is possible to calculate the losses of the devices. Losses in power switches primarily encompass conduction losses, switching losses, and gate driver losses. SiC MOSFET are used as an example for further details.

2.3.1 Conduction Loss

The conduction loss is calculated as shown in (4).

$$P_1 = I_D^2 * R_{DS(on)} * D \tag{4}$$

where I_D is the SiC MOSFET drain current, $R_{DS(on)}$ is the SiC MOSFET drain-source on-resistance and D is the SiC MOSFET duty cycle.

2.3.2 Turn-on and Turn-off Losses

The turn-on or turn-off loss is calculated as shown in (5).

$$P_2 = \frac{V_{DS}I_{out}}{2}tf_s \tag{5}$$

where V_{DS} is the SiC MOSFET drain voltage; I_{out} is the constant current source during SiC MOSFET turn-on or turn-off, t is the turn-on or turn-off loss time and f_s is the switching frequency.

2.3.3 Driving Loss

The driving loss is calculated as shown in (6).

$$P_3 = V_{GS}Q_Gf_s \tag{6}$$

where V_{GS} is the SiC MOSFET drive voltage; Q_G is the amount of all charges provided during the SiC MOSFET turn-on period.

The MSC015SMA070B has a lower loss than the IRGP6690DPbF under the operating condition of the same switching frequency obtained by (4), (5), (6).

3. Experimental Verification and Analysis

3.1 Fixed Load Experiment

To validate the feasibility of the proposed strategy, an experimental prototype of the MPPT converter was designed and manufactured, as illustrated in Fig. 5. The primary controller used was the DSP TMS320F280025, with a switching frequency set at 20kHz. A series of experiments were conducted on the four converter structures mentioned in section 2.3.
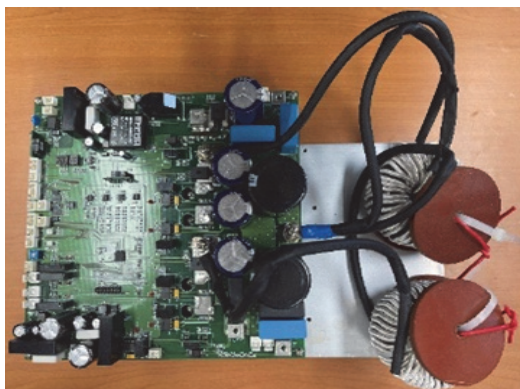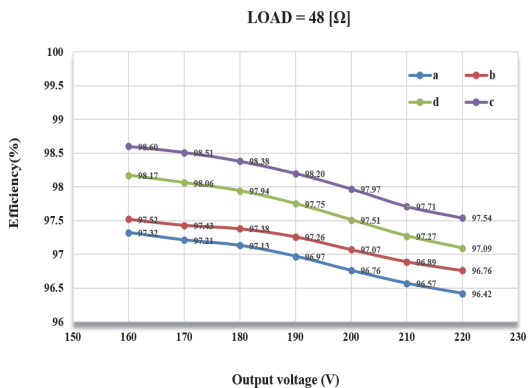
Initially, with an input voltage of 160V and a load of 48Ω, the output voltage was varied by adjusting the duty cycle, effectively modifying the output power. The efficiency is shown in Fig. 6.

Similarly, with an input voltage of 160V and loads of 24Ω and 16Ω, the operating states of the four circuits were modified by adjusting the duty cycle. The resulting efficiencies are depicted in Fig. 7.

From the efficiency analysis charts above, it is evident that the efficiency of (c) is the highest. However, as indicated in Table 1,

Fig. 5 Experimental prototype
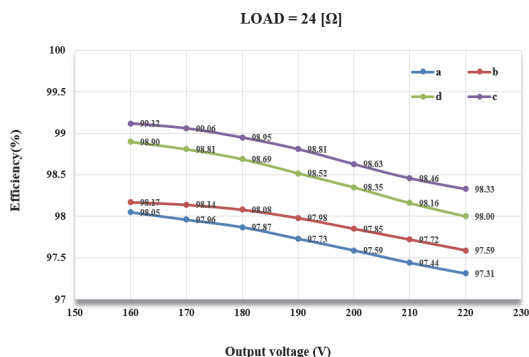
(a) Efficiency when the load is 24 Ω
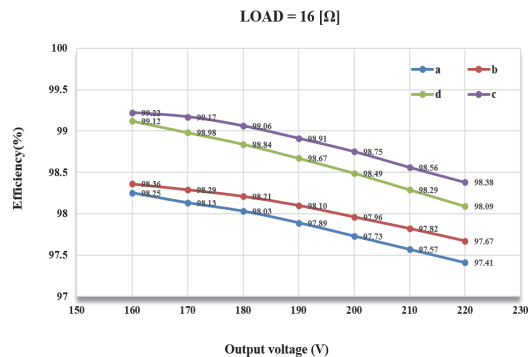
(b) Efficiency when the load is 16 Ω

Fig. 7 Efficiency when the load is 24 Ω and 16 Ω respectively

Fig. 6 Efficiency when the load is 48 Ω

the cost of SiC MOSFET is approximately four times that of Si IGBT. Therefore, for a balanced consideration of both efficiency and

Efficiency comparison between (a) and (d) (load = 48Ω)

Fig. 8 Efficiency comparison when the load is 48 Ω

Efficiency comparison between (a) and (d) (load = 24Ω)

(a) Efficiency comparison when the load is 24Ω

Efficiency comparison between a and d(load=16Ω)

(b) Efficiency comparison when the load is 16Ω

Fig. 9 The efficiency difference between under different voltage levels with loads of 24Ω and 16Ω

cost-effectiveness, choosing the proposed hybrid synchronous converter structure (d) is more advantageous.

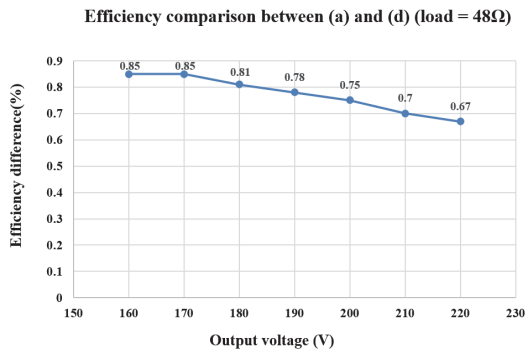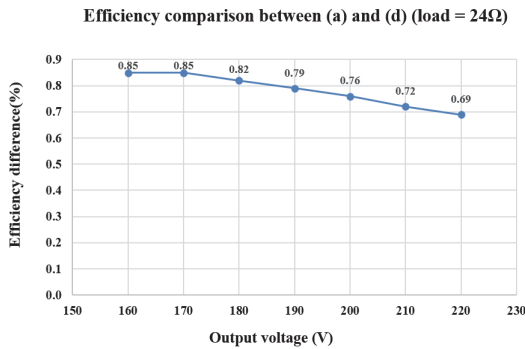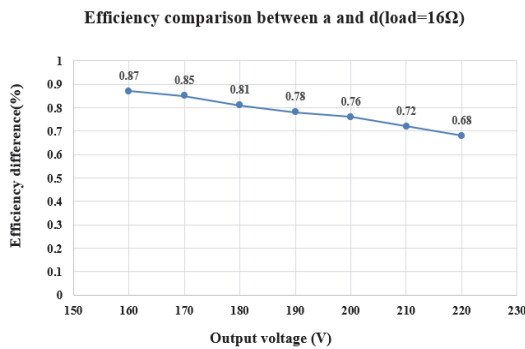Analyzing the efficiency difference between different voltage levels with loads of 48Ω, 24Ω, and 16Ω, the results are presented in Fig. 8 and Fig. 9.

The efficiency difference ranges from 0.65% to 0.9%, and it gradually decreases as the output voltage increases. In other words, with a larger duty cycle, the efficiency difference becomes smaller.

3.2 Fixed Duty Cycle Experiment

Compare the experimental efficiency of the converter (a) based on the Si IGBT structure in Section 2.3 with the proposed (d) at an output power of 0.5kW-3kW. The input voltage is 240V and the output voltage is 360V, which means the fixed duty cycle D is 0.33. The experimental efficiency is shown in Fig. 10.

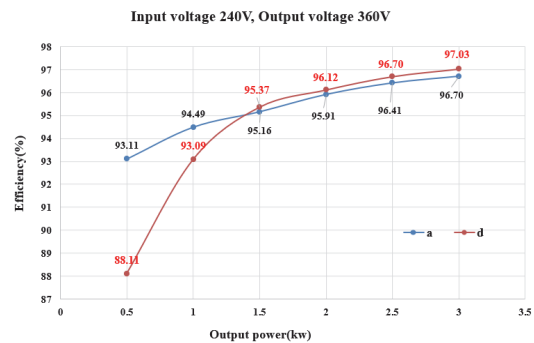**Input voltage 240V, Output voltage 360V**

Fig. 10 Experimental efficiency when the input voltage is 240V and the output voltage is 360V

From Fig. 10, it can be observed that, with a fixed duty cycle D of 0.33 and an output power lower than 1.5kW, the efficiency of (a) can be significantly higher than that of (d). When the input and output voltages are relatively high and remain constant, but the output power is lower, the current passing through the SiC MOSFET is reduced. Under these conditions, the influence of the SiC MOSFET's characteristics results in higher losses.

Therefore, under the aforementioned conditions, a change in the control strategy for the SiC MOSFET is necessary. When the output power is less than 1.4kW, synchronous control is not applied, and the current flows through the parasitic diode of the SiC MOSFET. The experimental efficiency is shown in Fig. 11.

The Fig. 11. clearly demonstrates a substantial enhancement in system efficiency within the 0.5kW-1.4kW range. Nonetheless, due to the higher resistance of the parasitic diode in the SiC MOSFET compared to the Si IGBT diode, the efficiency of (d) remains lower than that of (a).
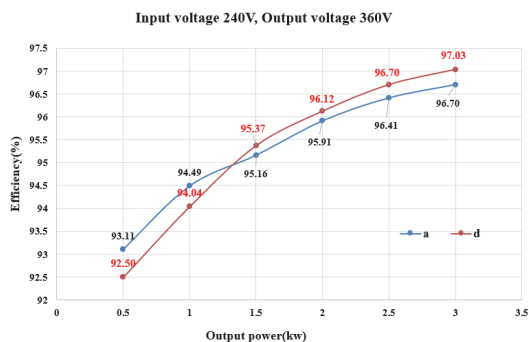
4. Conclusion

This research aims to improve the efficiency and reduce costs of solar cell photovoltaic systems. To this end, a hybrid high-efficiency synchronous converter is proposed that combines Si IGBT and SiC MOSFET to achieve a balance between performance and economy. Research highlights the importance of selecting different switching devices and control strategies at different load and power levels to optimize efficiency and reduce system costs. This study provides useful information for improving the efficiency of solar grid-connected power conversion systems.

Acknowledgements

Fig. 11 Control improved experimental efficiency

References

[1] Raiker G A, Loganathan U. Current control of boost converter for PV interface with momentum-based perturb and observe MPPT[J]. IEEE Transactions on Industry Applications, 2021, 57(4): 4071-4079.

[2] Jae-Joon Kim, Ki-Hyun Pyo, Joon-Hyeok Jeon, Sin-Su Kyung, and Eun-Soo Lee, "Single SiC Switch based 8kW PV Boost Converters with

ZVZCS Operation Generation," THE TRANSACTIONS OF KOREAN INSTITUTE OF POWER ELECTRONICS, vol. 28, no. 3, pp. 231-239, 2023, DOI: 10.6113/TKPE.2023.28.3.231

[3] Jun-Gu Kim, Jae-Hyung Kim, Chung-Yuen Won, and Yong-Chae Jung, "Synchronous Soft Switching Boost Converter," in Power Electronics Conference, 2008, pp. 187-189.tt

[4] Kook-Sun Lee, Ick Choy, Ju-Yeop Choi, Jinung An, and Dong-Ha Lee, "Efficiency analysis of the boost converter for compact solar array system," in 한국태양에너지학회 학술대회논문집, 2009, pp. 388-393.

[5] Jahan H K. A new transformerless inverter with leakage current limiting and voltage boosting capabilities for grid-connected PV applications[J]. IEEE Transactions on Industrial Electronics, 2019, 67(12): 10542-10551.

[6] Iqbal A, Bhaskar M S, Meraj M, et al. Closed-loop control and boundary for CCM and DCM of nonisolated inverting N× multilevel boost converter for high-voltage step-up applications[J]. IEEE Transactions on Industrial Electronics, 2019, 67(4): 2863-2874.

[7] Pai K J. Development and Implementation of a DCM Boost Converter With Multilayer Stacked Circuits Achieving High Voltage Gain[J]. IEEE Transactions on Industrial Electronics, 2023.

[8] Foroozeshfar R, Adib E. Three-phase ripple free DCM boost converter with low THD[J]. IET Power Electronics, 2019, 12(1): 120-128.

[9] Lee S W, Do H L. High-efficiency soft-switching step-up DC–DC converter derived from a synchronous boost converter[J]. IET Power Electronics, 2019, 12(7): 1662-1669.

[10] Zhiyong Dong,and Gyubum Joung. "Soft switched Synchronous Boost Converter for Battery Dischargers." Journal of Advanced Smart Convergence 9.2 (2020): 105-113.

[11] Yo-Han Jang, Jeong-Ho Ahn, Jung-Hae Choi, and Jae-Jung Yun, "A Study on the Synchronous Boost Converter Based on the GaN FET," Journal of the Korean Institute of Illuminating and Electrical Installation Engineers, vol. 33, no. 5, pp. 41-47, 2019, DOI: 10.5207/JIEIE. 2019.33.5.041

[12] Sankaranarayanan V, Gao Y, Erickson R W, et al. Online efficiency optimization of a closed-loop controlled SiC-based bidirectional boost converter[J]. IEEE Transactions on Power Electronics, 2021, 37(4): 4008-4021.

[13] Rogina M R, Rodriguez A, Vazquez A, et al. Improving the efficiency of SiC-based synchronous boost converter under variable switching frequency TCM and different input/output voltage ratios[J]. IEEE Transactions on Industry Applications, 2019, 55(6): 7757-7764.

[14] Yin T, Xu C, Lin L, et al. A SiC MOSFET and Si IGBT hybrid modular multilevel converter with specialized modulation scheme[J]. IEEE Transactions on Power Electronics, 2020, 35(12): 12623-12628.

[15] Yin T, Lin L, Xu C, et al. A hybrid modular multilevel converter comprising SiC MOSFET and Si IGBT with its specialized modulation and voltage balancing scheme[J]. IEEE Transactions on Industrial Electronics, 2021, 69(11): 11272-11282.